NASA Technical Memorandum 87143

Molten Salt Corrosion of SiC: Pitting Mechanism

N.S. Jacobson and J.L. Smialek
Lewis Research Center
Cleveland, Ohio

Prepared for the
One hundred sixty-eighth Meeting of the Electrochemical Society
Las Vegas, Nevada, October 13-18, 1985

NASA

MOLTEN SALT CORROSION OF SiC: PITTING MECHANISM

N.S. Jacobson and J.L. Smialek
National Aeronautics and Space Administration
Lewis Research Center
Cleveland, Ohio 44135

SUMMARY

Thin films of Na_2SO_4 and Na_2CO_3 at 1000 °C lead to severe pitting of sintered α-SiC. These pits are important as they cause a strength reduction in this material. The growth of product layers is related to pit formation for the Na_2CO_3 case. The early reaction stages involve repeated oxidation and dissolution to form sodium silicate. This results in severe grain boundary attack. After this a porous silica layer forms between the sodium silicate melt and the SiC. The pores in this layer appear to act as paths for the melt to reach the SiC and create larger pits.

INTRODUCTION

Silicon carbide shows particular promise as a high temperature structural material (ref. 1). In gas turbine, chemical reactor, and heat exchanger applications, this material may be exposed to molten salts. Evidence has been accumulating which indicates that SiC is quite susceptible to molten salt corrosion (refs. 2 to 7). This paper summarizes some of our work in this area and also presents some current ideas on corrosion pitting in SiC.

The starting material was a commercially available sintered α-SiC,* which shows particular promise for future applications (ref. 8). This material contains approximately 3 percent free carbon, in the form of inclusions a few microns in diameter. Specimens were coated with Na_2CO_3 or Na_2SO_4 and placed in a furnace at 1000 °C. Unless otherwise noted, all specimens were coated with approximately 2.5 mg salt/cm^2. It has been shown that basic molten salts readily attack SiC by dissolution of the protective silica scale to form sodium silicate (ref. 4). Thin films of Na_2CO_3 with a flowing 0.01 percent CO_2-O_2 atmosphere directly dissolve the SiO_2 film and lead to corrosion. Thin films of Na_2SO_4 with flowing air behave similarly. Surprisingly, Na_2SO_4 with a flowing 0.01 percent SO_3-O_2 atmosphere--a more acidic system--also corrodes this material. This is due to locally basic conditions at the Na_2SO_4/SiO_2 interface, promoted by free carbon in the sintered α-SiC.

In each of the three salt systems studied, the reaction occurs primarily in the first 5 hr. Corrosion products consist of both SiO_2 and $Na_2O{\cdot}x(SiO_2)$ (ref. 5). The major feature of these reactions is that consumption of the SiC substrate does not occur with a uniform material recession, but with a more localized pitting attack. The corrosion products can be easily removed with a 10 percent HF/H_2O solution. This solution does not attack the SiC substrate and thus allows examination of the corroded microstructure. Figure 1(a) is a surface view before corrosion, figure 1(b) is a surface view after Na_2CO_3

---

*Carborundum Co., Niagara Falls, NY.

corrosion with the products removed by HF. Note the pitted structure with the large crater-like pit in the center.

The surface and processing flaws in a ceramic have a major influence on its strength. These flaws may be fracture origins--when the ceramic is stressed they act like stress concentrators which result in failure strengths inversely proportional to the size of the flaw. Thus, the surface corrosion pits have a major effect on the strength of SiC (ref. 6). This is presented in figure 2, which shows the strengths of the as-received SiC bars and the strengths after corrosion by each of the three salt systems. In order to pin the strength reductions to corrosion pitting, extensive fractography was done. In most cases the fracture origin was due to corrosion pits (ref. 6). Examples are shown in figures 3 and 4 - note the characteristic radial lines of the fracture origin pointing toward the corrosion pit.

PITTING MECHANISM

The primary problem then is to understand how the corrosion pits form. The focus here is on the Na_2CO_3/CO_2 system. This basic salt directly attacks the SiO_2 layer and the mechanism of Na_2CO_3 corrosion of SiC is fairly well understood (ref. 5). The goal here is to relate the mechanism of product formation to mechanism of pit formation. Consider first the mechanism of product formation. A kinetic curve at 1000 °C is shown in figure 5. This curve was generated by chemical analysis of the corrosion products after various time intervals. A water leach removes the silicates for analysis; an HF leach removes the silica for analysis (ref. 4). The Na_2CO_3 is consumed in the first 0.25 hr of the reaction and is not shown in figure 5. The important point from this kinetic curve is that the $Na_2O{\cdot}x(SiO_2)$ peaks in the first 0.25 hr. This is very likely due to repeated oxidation and dissolution:

$$SiC + \frac{3}{2} O_2 = SiO_2 + CO \qquad (1)$$

$$xSiO_2 + Na_2CO_3 = Na_2O{\cdot}x(SiO_2) + CO_2 \qquad (2)$$

After the first 0.5 hr a stable SiO_2 film forms on the SiC and a layered sodium silicate/silica/silicon carbide structure develops. A water leach removes the outer silicate layer and reveals the silica layer in its early stages of development. This is shown in figure 6. The lower left hand corner of this photomicrograph shows a region where the SiO_2 layer had spalled revealing the pitted SiC substrate. Note the pores in the SiO_2 layer - which appear to extend to the SiC. These pores probably form when CO and CO_2 escape from the oxidation of SiC and the C inclusions. Figure 5 shows that SiO_2 increases after 0.5 hr at a rate much faster than simple protective oxidation (ref. 5). The pores in this layer may be oxygen paths for this nonprotective oxidation. In addition, figure 5 suggests that $Na_2O{\cdot}x(SiO_2)$ decomposes. This may occur in the low oxygen regions of the melt as follows:

$$\underline{Na_2O}{\cdot}x(SiO_2) = x(SiO_2) + 2\,Na + \frac{1}{2} O_2 \qquad (3)$$

Thus the silica forms both by nonprotective oxide growth and $Na_2O{\cdot}x(SiO_2)$ decomposition. After long times the lower silica layer becomes dense and quite

thick. This is shown in figure 7. This dense, protective silica layer seals off the SiC from further attack.

As the product layers become thicker, the pitting attack of the SiC substrate becomes more severe. Figure 8 shows a time sequence of pit formation. In each case the corrosion products were removed by an HF treatment. The 0.25 hr microstructure was formed by repeated oxidation and dissolution--it had a layer of sodium silicate directly on it. The SiC substrate shows primarily grain boundary attack, but also some intragranular attack which was very likely initiated on crystal defect sites. This is simply an "etching type" attack--where the higher energy sites are attacked first (ref. 9). Some of the small pits in this structure are very likely due to oxidation of the carbon inclusions in these pits. In some instances it appears the entire grain had been pulled out. Note also the grain boundary film--this may be important in the attack process. The 1 hr specimen had a layer of porous silica on it. This specimen also shows extensive grain boundary attack and some intragranular attack. However, now the pits are deeper and have a more crater-like appearance. Finally the 5 hr sample shows still larger craters. An overall view of the specimen shows the craters tend to be localized. These deep craters are important because some may be large enough to act as fracture origins.

Comparing figure 6 to figures 8(b) and (c) suggest that the pores in the lower silicon layer allow the melt to penetrate this layer and attack localized areas. Figures 9 and 10 illustrate this pore-pit correlation more clearly. This specimen was given a coating of 4.1 mg Na_2CO_3/cm^2, which tended to produce severe pitting along the edges after only 1 hr at 1000 °C. After corrosion, the sample had a dense, glassy product layer. Removing the sodium silicate with a water treatment revealed the pores shown in figures 9 and 10. Looking down these pores indicates that they are directly above a pit in the SiC. In both figures, the SiC grains can be seen in the bottom of a pit.

After 0.25 hr, the melt which penetrates these pores is primarily $Na_2O \cdot x(SiO_2)$. Nonetheless, as long as the local melt composition at the pit bottom does not exceed the phase diagram liquidus at $Na_2O \cdot 3.65(SiO_2)$, (ref. 10) the oxidation-dissolution process can continue to consume the SiC. Indeed, thin films of $Na_2O \cdot 1(SiO_2)$ readily attack SiC at 1000 °C. It should be noted that not all the silica which forms is dissolved by the melt - some adds to the thick silica layer shown in figure 7. Nonetheless evidence does suggest that penetration points in this layer allow the melt to reach the carbide and create localized, crater-like pits.

CONCLUSION

In summary, thin salt films of Na_2CO_3 and Na_2SO_4 cause severe corrosion pitting of sintered α SiC at 1000 °C. These corrosion pits can act as fracture origins and thus are responsible for corrosion attack strength decreases in this material after corrosion. In the Na_2CO_3 case, the first 0.25 hr of reaction are due to repeated overall SiC oxidation and dissolution of the oxide to sodium silicate. This leads to extensive grain boundary attack of the SiC substrate. After 0.25 hr a porous silica layer forms between the SiC and sodium silicate melt. This allows the melt access to the SiC in specific areas and localized crater-like pits form. These larger pits are of the greatest concern, because they can lead to a loss in strength of the SiC.

REFERENCES

1. H.B. Probst, Am. Ceram. Soc. Bull., 59, 206 (1980).

2. R.E. Tressler, M.D. Meiser, and T. Yonushonis, J. Am. Ceram. Soc., 59, 278 (1976).

3. M.K. Ferber, J. Ogle, V.J. Tennery, and T. Henson, J. Am. Ceram. Soc., 68, 191 (1985).

4. N.S. Jacobson and J.L. Smialek, J. Am. Ceram. Soc., 68, 432 (1985).

5. N.S. Jacobson, J. Am. Ceram. Soc., in press, (1985).

6. J.L. Smialek and N.S. Jacobson, "Mechanism of Strength Degradation for Hot Corrosion of α-SiC," National Aeronautics and Space Administration, Washington, D.C., NASA TM-87052 (1984).

7. N.S. Jacobson, C.A. Stearns, and J.L. Smialek, "Burner Rig Corrosion of SiC at 1000 °C," National Aeronautics and Space Administration, Washington, D.C., NASA TM-87061, (1985).

8. C. Belleau, W.L. Ehlers, and F.A. Hagan, "Materials Review for Improved Automotive Gas Turbine Engines," NASA CR-159673, 1978.

9. G.L. Kehl, "The Principles of Metallographic Laboratory Practice," pp. 60-79, McGraw-Hill, New York, (1949).

10. W.D. Kingery, H.K. Bowen, and D.R. Uhlmann, "Introduction to Ceramics," p. 359, Wiley, New York, (1976).

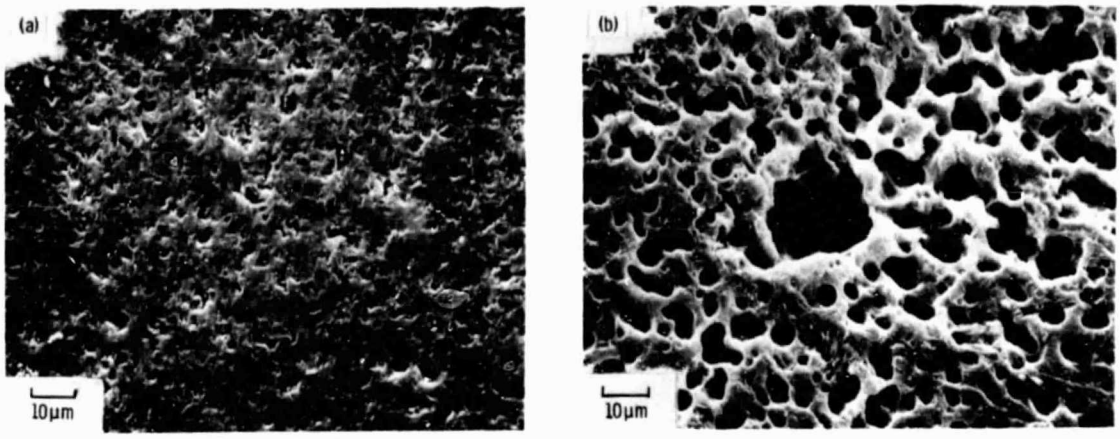

Figure 1. - Sintered α-SiC (a) 15μm surface finish prior to corrosion testing (b) After 48 hrs Na_2CO_3/CO_2 corrosion products removed with HF.

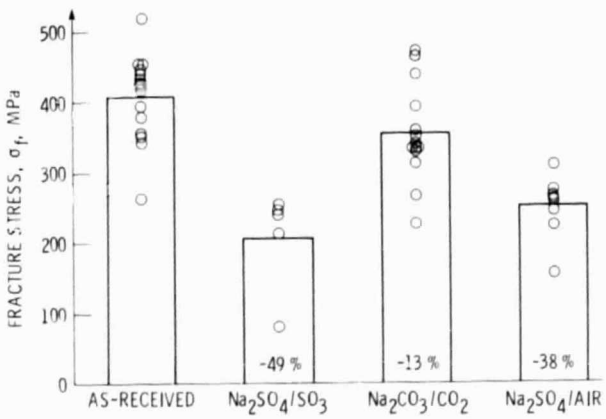

Figure 2. - Effect of 1000 °C/48 hr hot corrosion on 4-pt bend strength of α-SiC; samples ground to 15 μm finish before strength test.

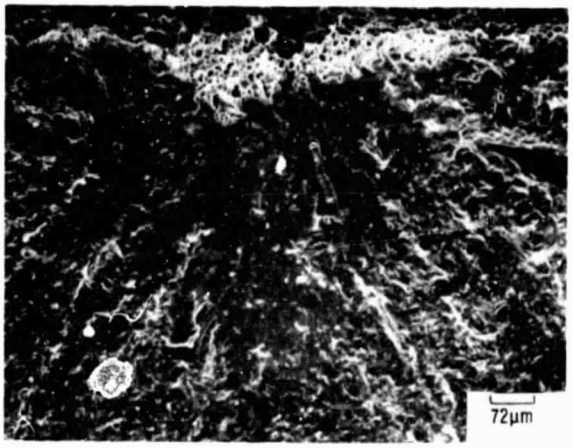

Figure 3. - Corrosion pit fracture origin after Na_2SO_4/SO_3 corrosion -- products removed with HF (σ_f = 190 MPa).

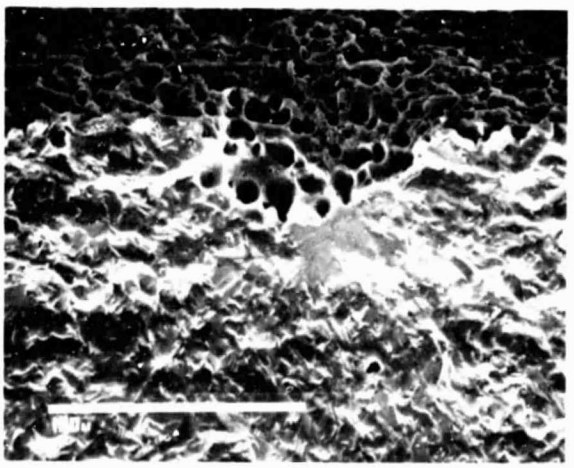

Figure 4. - Corrosion pit fracture origin after Na_2CO_3/CO_2 corrosion -- products removed with HF (σ_f = 334 MPa).

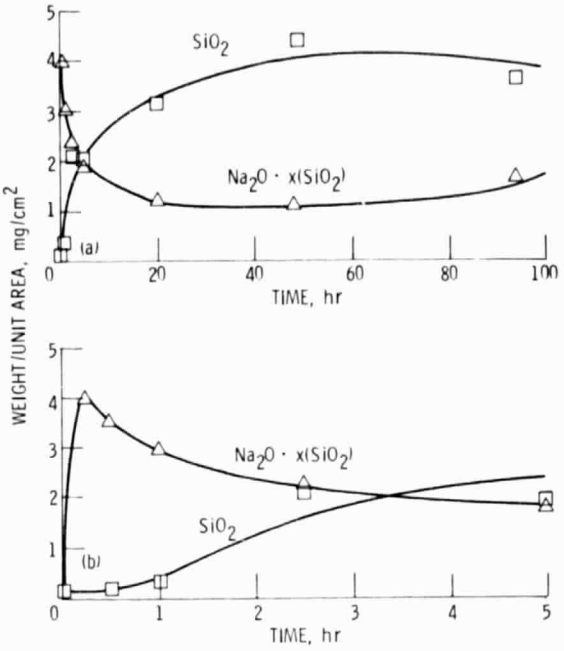

Figure 5. - Product evolution for Na_2CO_3/CO_2 corroded SiC (a) and enlargement of first 5 hr (b).

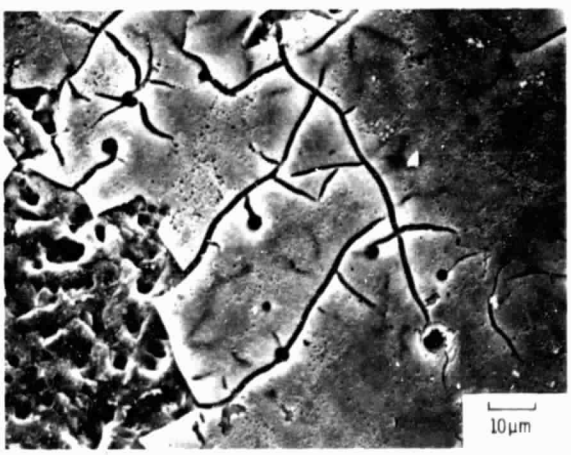

Figure 6. - Lower silica after 0.5 hr (outer silicate layer removed with water).

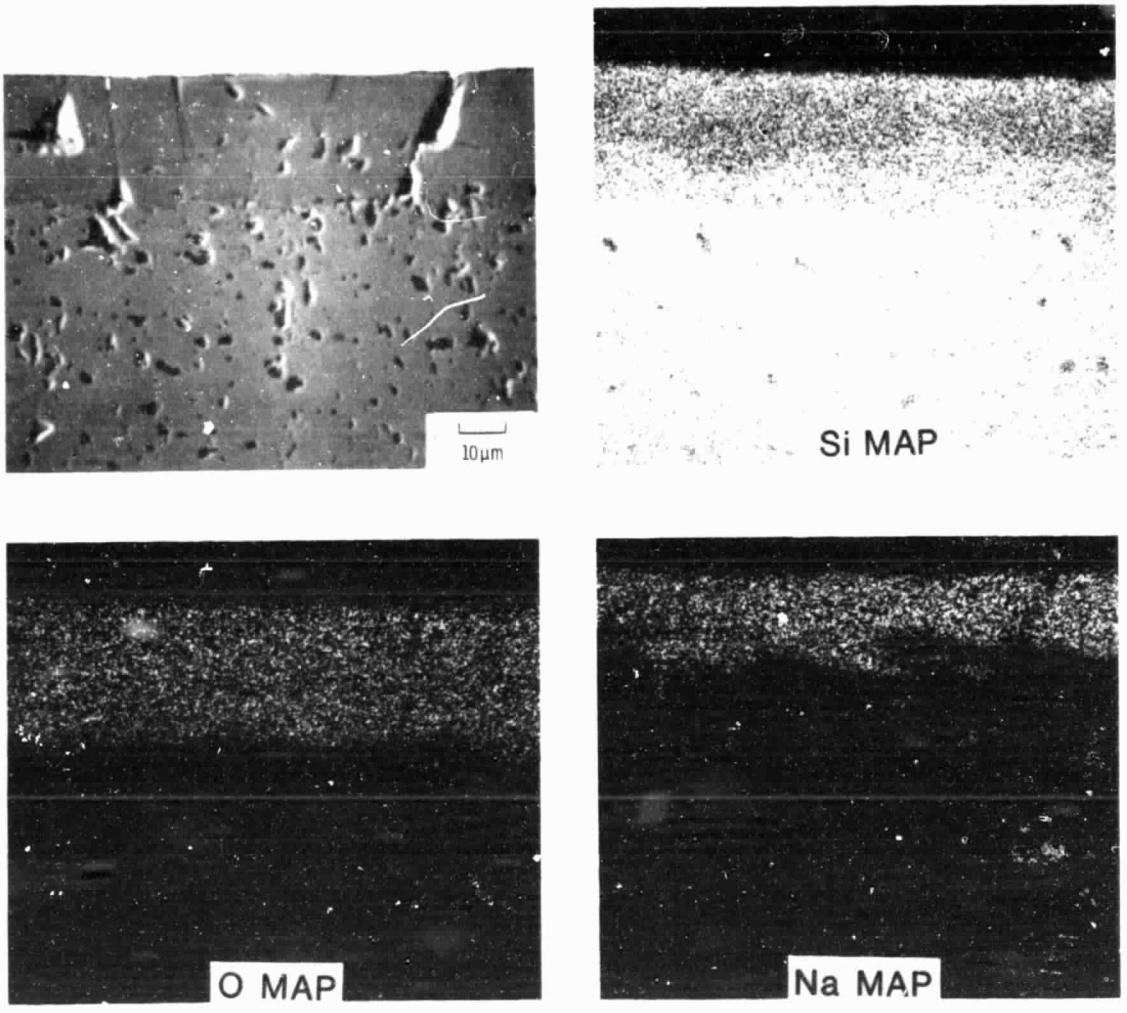

Figure 7. - Cross section of Na_2CO_3/CO_2 corroded SiC - 48 hrs.

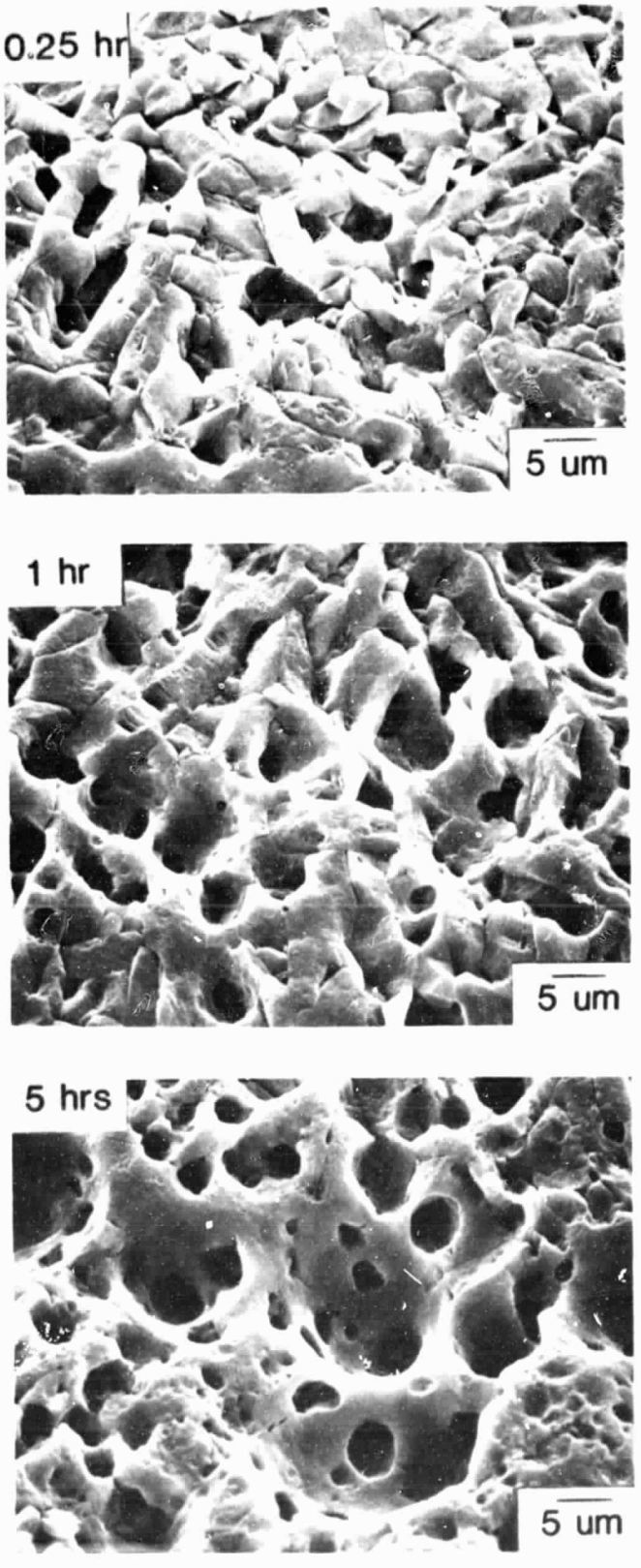

Figure 8. - Time sequence showing evolution of pits (corrosion products removed by HF).

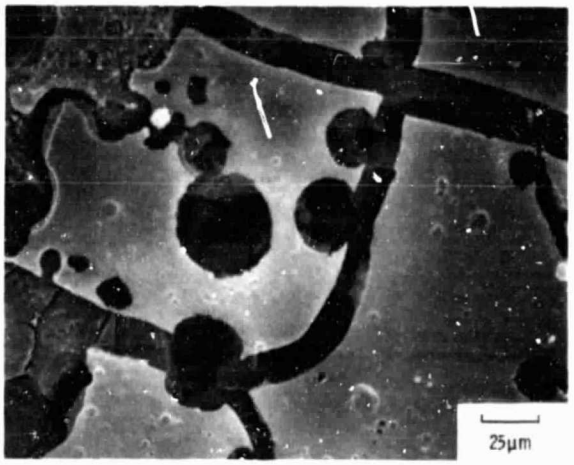

Figure 9. - Inner silica layer over pitted SiC after 1 hr (outer silicate layer removed with water). Note pores in silica extending to pits in SiC.

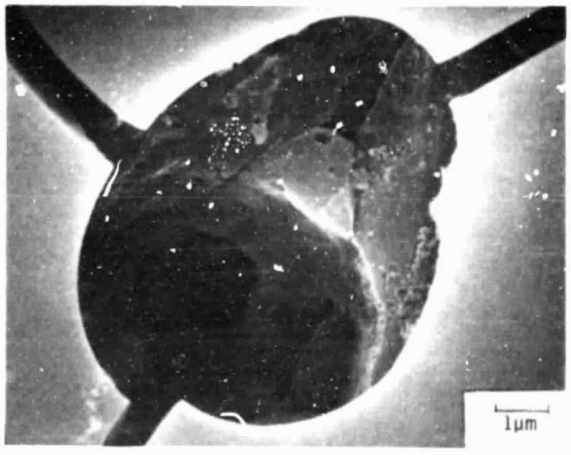

Figure 10. - Detail of specimen shown in fig. 9, showing a pore in the silica providing a path to a SiC pit.

1. Report No.	2. Government Accession No.	3. Recipient's Catalog No.
NASA TM-87143		

4. Title and Subtitle	5. Report Date
Molten Salt Corrosion of SiC: Pitting Mechanism	
	6. Performing Organization Code: 533-05-12
7. Author(s): N.S. Jacobson and J.L. Smialek	8. Performing Organization Report No.: E-2770
	10. Work Unit No.
9. Performing Organization Name and Address: National Aeronautics and Space Administration, Lewis Research Center, Cleveland, Ohio 44135	11. Contract or Grant No.
	13. Type of Report and Period Covered: Technical Memorandum
12. Sponsoring Agency Name and Address: National Aeronautics and Space Administration, Washington, D.C. 20546	14. Sponsoring Agency Code

15. Supplementary Notes

Prepared for the One hundred sixty-eighth Meeting of the Electrochemical Society, Las Vegas, Nevada, October 13-18, 1985.

16. Abstract

Thin films of Na_2SO_4 and Na_2CO_3 at 1000 °C lead to severe pitting of sintered α-SiC. These pits are important as they cause a strength reduction in this material. The growth of product layers is related to pit formation for the Na_2CO_3 case. The early reaction stages involve repeated oxidation and dissolution to form sodium silicate. This results in severe grain boundary attack. After this a porous silica layer forms between the sodium silicate melt and the SiC. The pores in this layer appear to act as paths for the melt to reach the SiC and create larger pits.

17. Key Words (Suggested by Author(s))	18. Distribution Statement
Corrosion; Pitting; SiC; Molten salt	Unclassified - unlimited STAR Category 27

19. Security Classif. (of this report)	20. Security Classif. (of this page)	21. No. of pages	22. Price*
Unclassified	Unclassified		

*For sale by the National Technical Information Service, Springfield, Virginia 22161